CCS Chemistry

RESEARCH ARTICLE

Received: June 19, 2019 | Accepted: Aug. 20, 2019 | Published: Oct. 1, 2019

Solvent-Assisted Supramolecular Assembly of Cyclotetrasiloxane–Functionalized Alkynylplatinum(II) Terpyridine Complexes

Ho-Leung Au-Yeung, Sammual Yu-Lut Leung & Vivian Wing-Wah Yam*

Institute of Molecular Functional Materials [Areas of Excellence Scheme, University Grants Committee (Hong Kong)] and Department of Chemistry, The University of Hong Kong, Pokfulam Road, Hong Kong (China)

**Corresponding author: wwyam@hku.hk*

Cite this: *CCS Chem.* **2019**, *1*, 464–475

Our present study demonstrated and explored the solvent effects on the association mechanism of the supramolecular nanomaterials in a series of cyclotetrasiloxane-appended alkynylplatinum(II) terpyridine complexes. Through the delicate balance of molecular interactions, some of these complexes were found to exhibit molecular association properties, with possible morphological transformation in response to solvent polarities. Twisted fibrils and nanoplates were apparent in aqueous and nonpolar media, respectively. Following the investigation of their molecular packing via powder X-ray diffraction and selected area electron diffraction experiments, we proposed a packing conformation, as follows: These nanostructure fabrications demonstrated to have been assisted by the presence of Pt···Pt interactions, in which the associated dramatic and rich spectroscopic response proceeded through mechanistic tracking of the assembly process. Further, nucleation and elongation modeling studies illustrated a solvent dependence of the association mechanism, with cooperative and isodesmic growth mechanism revealed in aqueous and apolar conditions, respectively.

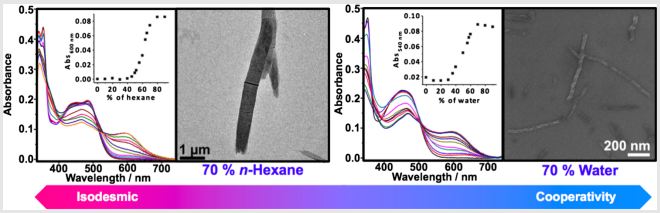

Keywords: supramolecular, cyclotetrasiloxane, platinum, solvent effects, hydrophobic interaction, nanomaterial, metal–metal interactions, noncovalent interaction, supramolecular polymerization mechanism

Introduction

Platinum(II) complexes with d^8 electronic configuration are well-known to possess high stability and rich spectroscopic properties, associated with the formation of self-assembly of nanostructures.[1–25] In particular, square-planar platinum(II) complexes with sterically undemanding ligands are found to further exhibit special electronic properties and solid-state polymorphism.[1] From an earlier discovery of ground-state oligomerization in $[Pt(CN)_4]^{2-}$ complex[2–4] through the development of classical color of the Magnus' green salt[5] and solid-state platinum(II) polypyridines,[6,7] to the more recent supramolecular association of the platinum(II) terpyridine systems in solutions,[8–10] enormous attention has been focused on the exploration of the platinum(II) system

DOI: 10.31635/ccschem.019.20190041
CCS Chem. **2019**, *1*, 464–475

that exhibits Pt···Pt interactions, due to their drastic spectroscopic and luminescence changes, which correlate to the extent of the Pt···Pt separations.[3,4,6,7,11]

Beside, the design and construction of cubic or cyclic oligosiloxane functional materials have received much attention in recent decades.[26-32] In particular, cubic silsesquioxanes of general formula $Si_8O_{12}R_8$ have demonstrated numerous applications, partly due to their tailorable functional domains that contribute to their fascinating properties, including reactivity, solubility, thermal stabilities, mechanical properties, and other physical properties.[28,29] Meanwhile, the development of cyclic siloxanes in constructing nanobuilding blocks toward precisely controlled nanostructures with predictable properties is of growing interest.[26] Such silicon-containing macrocycles, also known as cyclosiloxanes, with general formula of $(R_2SiO)_n$ (abbreviated D_n),[30,31] exhibit processable organic substituents similar to that demonstrated in cubic silsesquioxanes, with peripheral units generally determining the chemical and physical properties of the cyclosiloxane derivatives.[30,31]

Despite the symmetric and well-defined structures of the cyclosiloxane derivatives that would allow them to serve as promising candidates for constructing supramolecular functional materials,[32] the utilization of the siloxane rings in constructing molecular precursors toward supramolecular chemistry has remained scarce. Attracted by the rich spectroscopic properties of the d^8 platinum(II) terpyridine system, as well as the possibility in manipulating the Pt···Pt and π–π stacking interactions toward the construction of distinct nanomaterials,[1-25] functional hybrid materials with molecular association behaviors could be constructed via the coupling of the platinum(II) moieties with the cyclotetrasiloxane domains. Such formation of supramolecular nanostructures leads to interesting spectroscopic and luminescence changes, which could potentially serve as a tracker and reporter for the supramolecular assembly processes, and the corresponding mechanistic studies. In view of this, we sought to conduct the following research: (1) Synthesize and characterize a series of cyclotetrasiloxane–functionalized alkynylplatinum(II) terpyridine complexes (Scheme 1). (2) Explore the supramolecular self-assembly behaviors of the complexes in various solvent compositions with the associated spectroscopic and luminescence changes. (3) Study the self-association mechanisms of the complexes.

Sterically bulky 3,3-dimethyl-substituted α-alkene was employed to synthesize the target-functionalized cyclotetrasiloxane ligand by hydrosilylation,[33] with heptamethyl cyclotetrasiloxane using Karstedt's catalyst to avoid the generation of the β-addition isomeric side product.[34] Cyclotetrasiloxane–functionalized complexes **1**–**6** were synthesized through Cu(I)-catalyzed reaction of the chloroplatinum(II) terpyridine precursor complex with the respective alkynes under inert atmosphere, followed by recrystallization to offer the pure complexes, which were well characterized by ^{1}H NMR spectroscopy, IR spectroscopy, fast atom bombardment mass spectrometry, and high-resolution electrospray ionization mass spectrometry. Their IR spectra exhibited

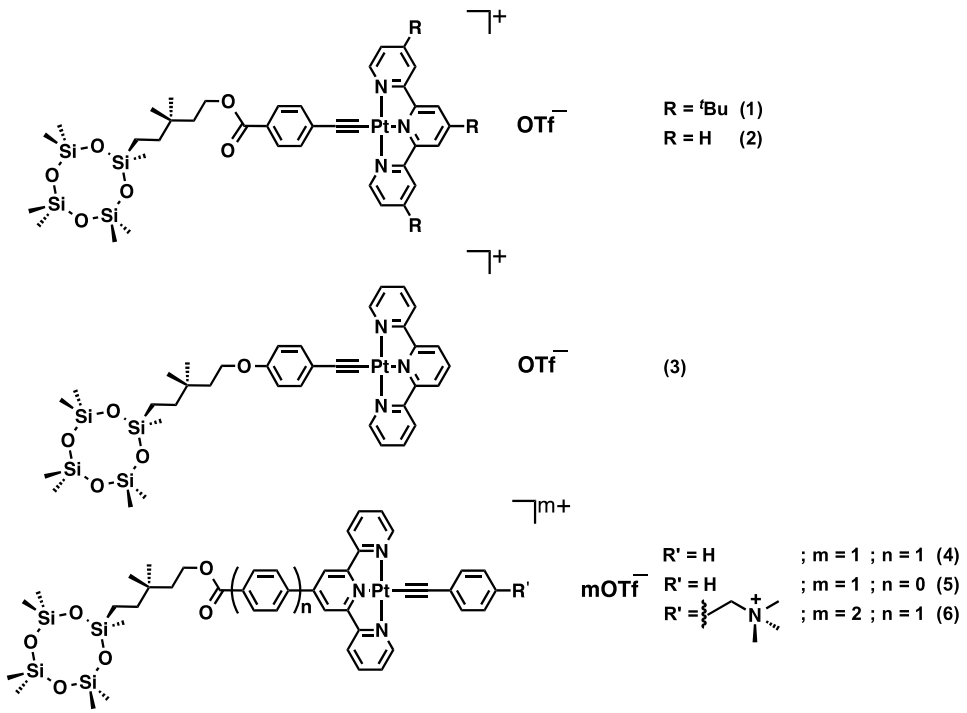

Scheme 1 | *Structures of alkynylplatinum(II) terpyridine complexes **1**–**6**.*

DOI: 10.31635/ccschem.019.20190041
CCS Chem. **2019**, *1*, 464–475

characteristic ν(Si–O) stretching mode at 1080–1111 cm^{-1}, typical of siloxane moieties, whereas the ν(C≡C) absorptions at 2122–2154 cm^{-1} were consistent with an alkynyl ligand in a terminal σ-coordination mode. All the complexes were found to exhibit moderate solubility in acetone and tetrahydrofuran (THF), except **2**, which exhibited only limited solubility in common organic solvents.

Results and Discussion

Among various complexes, complex **1**, substituted with sterically demanding tri-*tert*-butyl domains, represented our control compound, of which the Pt···Pt and/or π–π stacking interactions was hampered, thereby, making complex **1** a suitable candidate for exploring the basic photophysical properties of our series of synthesized complexes in their discrete monomeric form. Dissolution of **1** in THF yielded a clear yellow solution (Supporting Information Figure S1) that showed high- and low-energy absorption bands in the UV–vis absorption spectrum, as shown in Supporting Information Figure S2. The photophysical data of **1**–**6** are summarized in Supporting Information Table S1. The high-energy absorption band at ~ 300–350 nm is assigned to the intraligand [$\pi \rightarrow \pi^*$] transitions of alkynyl and terpyridine ligands, whereas the low-energy absorption band at ~ 390–450 nm is typical of the metal-to-ligand charge transfer (MLCT) [$d\pi(Pt) \rightarrow \pi^*(tpy)$] transition mixed with an alkynyl-to-terpyridine ligand-to-ligand change transfer (LLCT) character, commonly found in alkynylplatinum(II) terpyridine complexes.[6,35–38] In stark contrast to the tri-*tert*-butyl-substituted **1**, dissolution of the sterically undemanding complex **3** in THF gave a pale-orange solution. The corresponding electronic absorption spectrum revealed a much lower energy band at 520 nm, in a typical region where metal–metal-to-ligand charge transfer (MMLCT) transitions occurred,[6,35–38] indicative of the existence of Pt···Pt interactions arising from self-assembly of complex **3** in the THF medium. To further investigate this phenomenon, solvent-dependent electronic absorption studies were conducted. The results revealed a drastic color change from orange (THF) to yellow upon increasing the water composition to 30% (Supporting Information Figure S3), possibly indicating the occurrence of a deaggregation process. We inferred that it is likely that in the less-polar THF media, ground-state aggregation of **3** occurred, while raising the water composition improved the solvation, leading to a deaggregated state.[39,40] Interestingly, as the solvent polarity rising, it led to a further color change from yellow to red (80% water), accompanied by the restoration of the low-energy MMLCT absorption shoulder at ~ 520 nm with isosbestic points in the UV–vis absorption spectral traces, as depicted in Figure 1. This latter observation was brought about likely by the Pt···Pt and/or π–π interactions as a result of hydrophobic–hydrophobic interactions of the

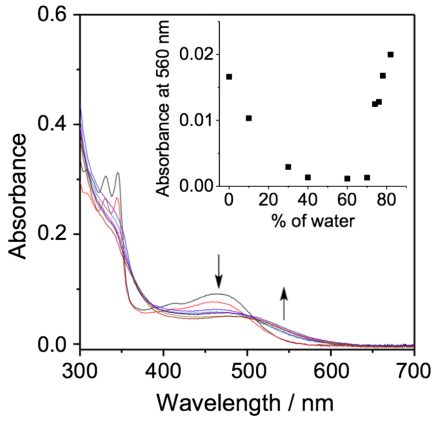

Figure 1 | *UV–Vis absorption spectral changes of **3** (2.8×10^{-5} M) in THF with increasing water content from 60% to 82%. The inset shows the absorbance at 560 nm as a function of solvent composition.*

alkynylplatinum(II) terpyridine and cyclotetrasiloxane moieties upon an increase in the nonsolvent content. The corresponding plot of the absorbance at ~ 560 nm against change in water content (Figure 1, inset) showed that critical water content of around 72% was required to trigger the growth of the MMLCT transition band, revealing the initiation of the aggregation process. Such drastic spectral changes revealed the aggregation–deaggregation–aggregation process upon solvent variation, demonstrating the aggregation ability of this class of complexes in both polar and nonpolar media. In contrast to **3**, similar solvent-dependent electronic absorption studies of **1** reveal only slight color and spectral changes upon addition of water (Supporting Information Figure S2), indicating the absence of significant aggregation behavior in response to changes in solvent polarity. Such observation suggested that the sterically bulky *tert*-butyl groups on **1** could effectively suppress and weaken the metal–metal and π–π stacking interactions, minimizing molecular aggregation.

Solvent-dependent studies of **3** revealed the exhibition of an initial molecular association process in THF. In order to avoid premature aggregation in interfering with the study of the assembly mechanism, another solvent, acetone, was used in place of THF for parallel solvent-dependent measurements. Similar trends, except the absence of the initial aggregation, were observed for **3** in acetone media (Supporting Information Figure S4). Subsequently, similar solvent-dependent studies in acetone were carried out for complexes **4**–**6**. Our results showed that all of them displayed significant spectroscopic changes in response to an addition of water, with the development of low-energy absorption tails, revealed from their corresponding electronic absorption spectra (Figures 2 and 3; Supporting Information Figures S5–S7), indicating the presence of Pt···Pt interactions.

DOI: 10.31635/ccschem.019.20190041
CCS Chem. **2019**, *1*, 464–475

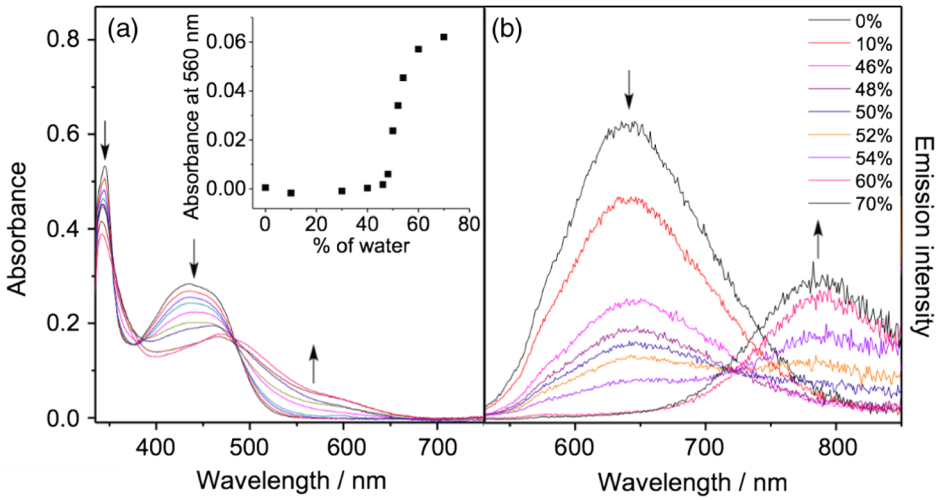

Figure 2 | *(a) UV–Vis absorption spectral changes of **4** (4.0×10^{-5} M) in acetone with increasing water content from 30% to 70%. (b) The corresponding corrected emission spectral changes in response to the changes in water composition from 0% to 70%.*

Further support for the self-association came from the corresponding emission studies of these platinum(II) complexes (Figures 2b and 3b), where solvent-dependent luminescence spectra of **5** reveal a drop of the ^{3}MLCT/^{3}LLCT emission band at ~ 680 nm, together with an emerging low-energy luminescence at 795 nm, upon increasing water content in the acetone solution (Figure 3b). Such red-shifted and enhanced luminescence at high water content could be attributable to a molecular association process, bringing the platinum moieties into proximity to facilitate the end-on overlap of the d_{z^2} orbitals on the platinum and an increase in the energy of the highest occupied molecular orbital,[12] thereby, accounting for the drastic color change. Such drastic color and spectroscopic changes indicate the presence of Pt···Pt and/or π–π stacking interactions as a result of reduced solvation in solvents of increased solvent polarity, which further suggests that such formation of aggregates could be stabilized by the formation of Pt···Pt and hydrophobic–hydrophobic interactions. These results further suggest that such formation of aggregates were stabilized by the formation of Pt···Pt and hydrophobic–hydrophobic interactions.

Similar observation on the development of MMLCT transition at high water content was also illustrated in the solvent-dependent luminescence studies of complex

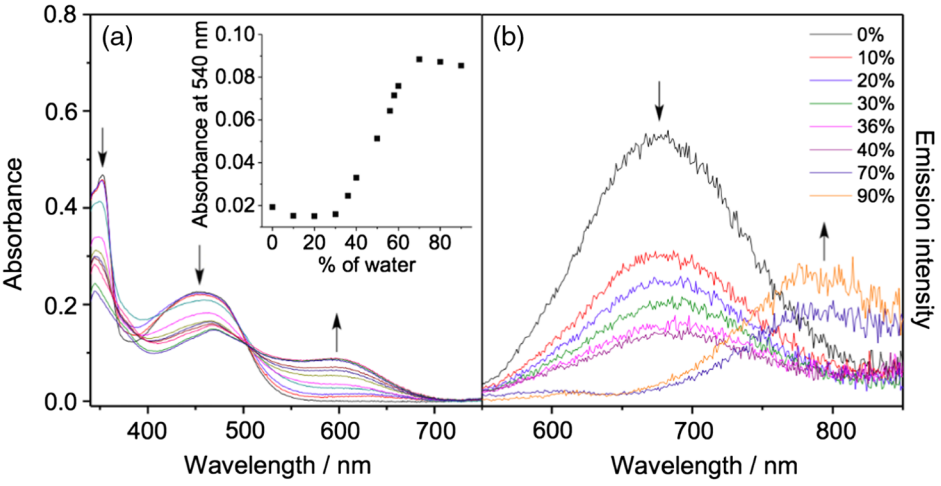

Figure 3 | *(a) UV–Vis absorption spectral changes of **5** (4.3×10^{-5} M) in acetone with increasing water content from 10% to 90%. (b) The corresponding corrected emission spectral changes in response to the changes in water composition from 0% to 90%.*

DOI: 10.31635/ccschem.019.20190041
CCS Chem. **2019**, *1*, 464–475

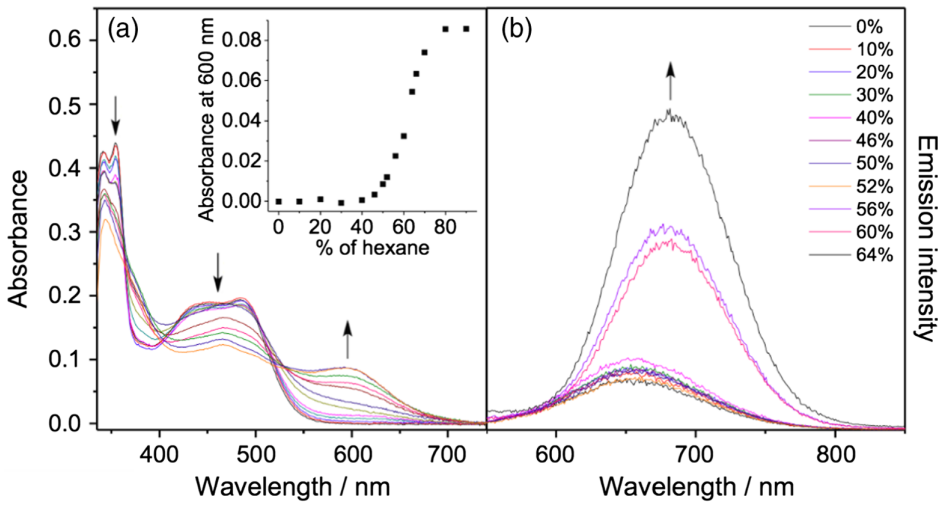

Figure 4 | *(a) UV–Vis absorption spectral changes of **5** (3.7×10^{-5} M) in acetone with increasing* n*-hexane content from 20% to 90%. (b) The corresponding corrected emission spectral changes in response to the changes in* n*-hexane composition from 0% to 64%.*

4 (Figure 2b), indicating the presence of Pt···Pt and/or π–π stacking interactions in polar media. In contrast, complex **6** was found to be nonemissive in aqueous media.

Solvent-Dependent Electronic Absorption and Luminescence Spectroscopy in Nonpolar Media

Following our demonstration that complexes **1**–**6** underwent aggregation in polar media due to the hydrophobic nature of the cyclosiloxane moieties, and further showing specifically in solvent-dependent studies that complex **3** tended to aggregate in THF media, unveiled the possibilities for the occurrence of molecular association in nonpolar solvents. In this regard, the self-assembly behaviors of **3**–**6** in nonpolar media were also explored to investigate the difference in the aggregation process among various solvent compositions.

Dissolution of complex **5** in acetone resulted in a yellow solution, which changed to red upon gradual addition of *n*-hexane, as depicted in Supporting Information Figure S8. The corresponding electronic absorption studies revealed a drop from high-energy MLCT absorption at ~ 470 nm with a concomitant uprise at the low-energy region of ~ 600 nm (Figure 4a), typically assigned to MMLCT transition, which was an indication of the

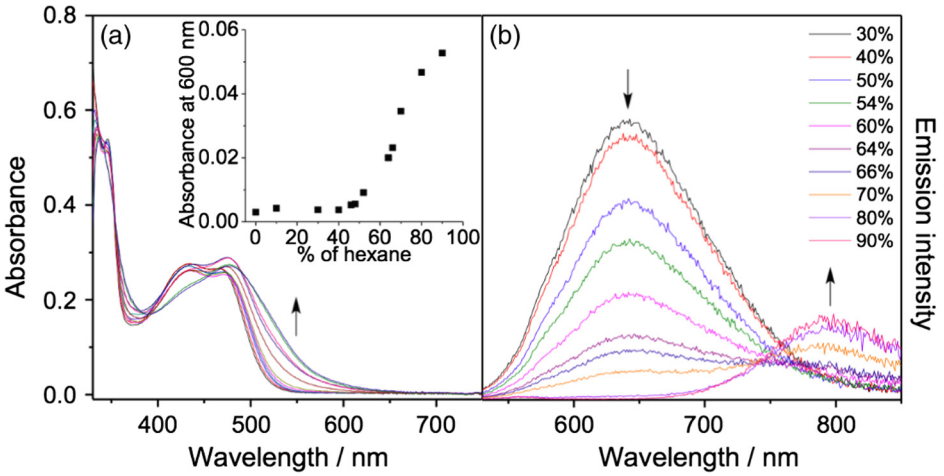

Figure 5 | *(a) UV–Vis absorption spectral changes of **4** (3.7×10^{-5} M) in acetone with increasing* n*-hexane content from 0% to 66%. (b) The corresponding corrected emission spectral changes in response to the change in* n*-hexane composition from 30% to 90%.*

DOI: 10.31635/ccschem.019.20190041
CCS Chem. **2019**, *1*, 464–475

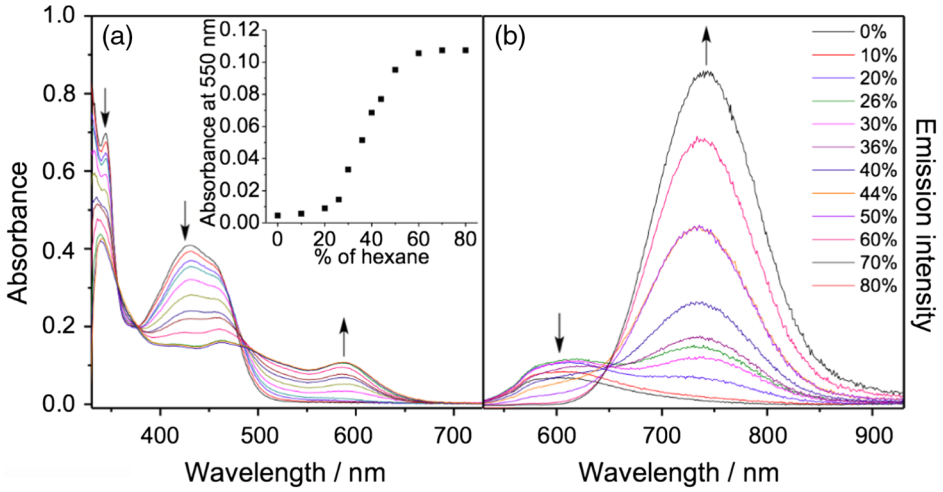

Figure 6 | *(a) UV–Vis absorption spectral changes of* ***6*** *(4.4 × 10^{-5} M) in acetone with increasing* n*-hexane content from 0% to 80%. (b) The corresponding corrected emission spectra in response to the change in* n*-hexane composition from 0% to 80%.*

formation of Pt···Pt and/or π–π stacking interactions. Corresponding emission studies further support the assignments, with luminescence enhancement and a slight red shift in emission maximum to ~ 685 nm upon *n*-hexane addition (Figure 4b). The enhanced emission of ^{3}MMLCT origin was derived from the molecular association and the formation of Pt···Pt and/or π–π stacking interactions in nonpolar media. To further reveal the presence of aggregated species, solvent-dependent ^{1}H NMR studies of **5** were also performed (Supporting Information Figure S9). Upon the successive addition of [D_{14}]*n*-hexane in [D_6]acetone, a gradual upfield shift, and broadening of proton signals corresponding to the terpyridine units were apparent, supporting the presence of molecular association in nonpolar media. Such formation of aggregated species in nonpolar media was attributable to the reduced solvation of the cationic complexes as a result of the addition of the nonsolvent. Similar phenomena were also observed with complexes **3**, **4,** and **6** (Figures 5 and 6; Supporting Information Figures S10 and S11), confirming their self-association in the nonpolar media.

Electron Microscopic Study on Self-Assembly Behavior

Electronic absorption and luminescence spectroscopy revealed the formation of aggregated species upon the variation of solvent compositions. In order to characterize the identities of these aggregated species, transmission electron microscopy (TEM) and scanning electron microscopy (SEM) were employed to probe the nanostructures under various solvent compositions. Complex **3**, which earlier demonstrated significant spectroscopic changes at high water composition (~ 70% water–acetone mixture), also revealed the framework of both left- and right-handed short-twisted fibrils with lengths and widths of ~ 300 and 30 nm, respectively, in TEM images (Figure 7a) under the same solvent mixture conditions. In contrast, TEM images of sterically demanding complex **1** did not reveal any distinct supramolecular architectures in similar solvent mixture (70% water in acetone) environment, indicating that the assembly process did not occur. These observations correlated with the spectroscopic results, revealing an effective suppression and weakening of the Pt···Pt and π–π stacking interactions upon introduction of sterically encumbered substituents, including *tert*-butyl moieties in complex **1**, that impeded the molecular association, even in the presence of hydrophobic driving forces. In addition, a similar electron microscopic examination was applied to complexes **4** and **5** (Figure 7c,d). Notably, electron micrographs of **4** and **5** also reveal the presence of both left- and right-handed twisted fibrils in 70% water–acetone mixture with similar dimensions of a few hundred nanometers long and ~ 40 nm wide, resembling those observed in **3**. Such findings further illustrated the lack of preference for a specific handedness in the self-assembly process and could be attributable to the absence of chiral centers in regulating the association process, leading to the formation of both left- and right-handed twisted fibrils in a random statistical distribution. The corresponding selected area electron diffraction (SAED) experiments on the twisted nanofibrils prepared from **4** and **5** (Supporting Information Figures S12 and S13) revealed diffraction rings with *d*-spacing of ~ 0.34 nm, confirming the involvement of metal–metal and/or π–π stacking interactions in their molecular packing.

Furthermore, supramolecular species of **3**–**5** in nonpolar media were also probed by electron microscopy to

DOI: 10.31635/ccschem.019.20190041
CCS Chem. **2019**, *1*, 464–475

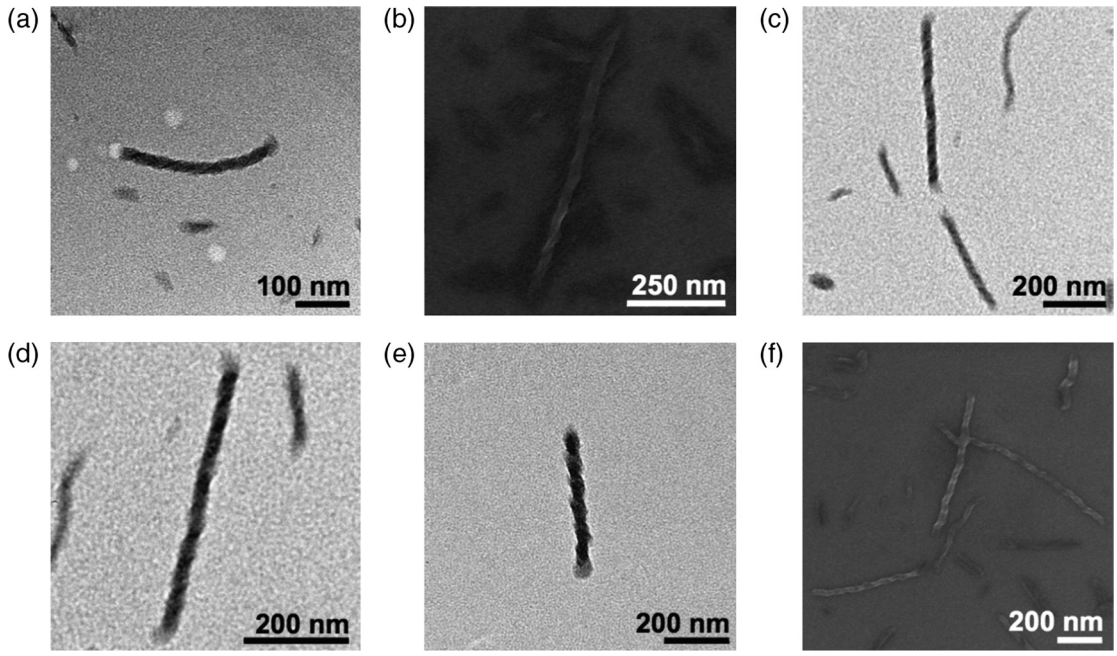

Figure 7 | *TEM and SEM images of the twisted fibrils prepared in 70% water–acetone mixture from (a, b)* ***3*** *(2 × 10^{-4} M); (c, d)* ***4*** *(2 × 10^{-4} M); and (e, f)* ***5*** *(2 × 10^{-4} M).*

explore their supramolecular assembly properties. In contrast to the aggregation process in aqueous media, TEM images of **3** in 70% *n*-hexane–acetone mixture revealed plate-like aggregates with dimensions within the micrometers range (Figure 8a). Interestingly, similar plate-like nanoaggregates were also apparent in the corresponding electron micrographs of complexes **4** and **5** under similar solvent compositions (70% *n*-hexane in acetone solution) (Figure 8b,c, respectively). TEM images of **4** also exhibited plate-like aggregates but with lengths of ~ 1 μm and widths in hundreds nm range(Figure 8b), whereas electron micrographs of **5** reveal the presence of uniform nanoplates with lengths and widths of ~ 1 μm and ~ 170 nm , respectively (Figure 8c). Notably, the corresponding SAED patterns of a single nanoplate prepared from **5** (Figure 9) revealed two sets of diffraction signals. The diffraction spots/arcs parallel to the nanoplate with *d*-spacing of ~ 0.32 nm revealed the presence of one-dimensional Pt···Pt and/or π–π stacking interactions along the long axis of the nanostructure, whereas the sets of diffraction spots perpendicular to the nanoplate corresponding to *d*-spacings of ~ 1.4 and 0.7 nm, revealed the molecular packing information perpendicular to the nanoplate long axis. The powder X-ray diffraction pattern of a dried film of **5** in *n*-hexane–acetone mixture revealed a series of evenly spaced Bragg peaks in the region of $2° < 2\theta < 30°$, indexed as (001), (002), (003), and (004) reflections. The *d*-spacings calculated are in a ratio of ~ 1:1/2:1/3:1/4, corresponding to ~ 2.81, 1.41, 0.94 and 0.70 nm, respectively, characteristic of a lamellar packing with a lattice parameter, *c* = 2.81 nm (Figure 9c),[41] and consistent with the SAED findings. Figure 10 illustrates the proposed structure of the nanoplates prepared from **5** in nonpolar

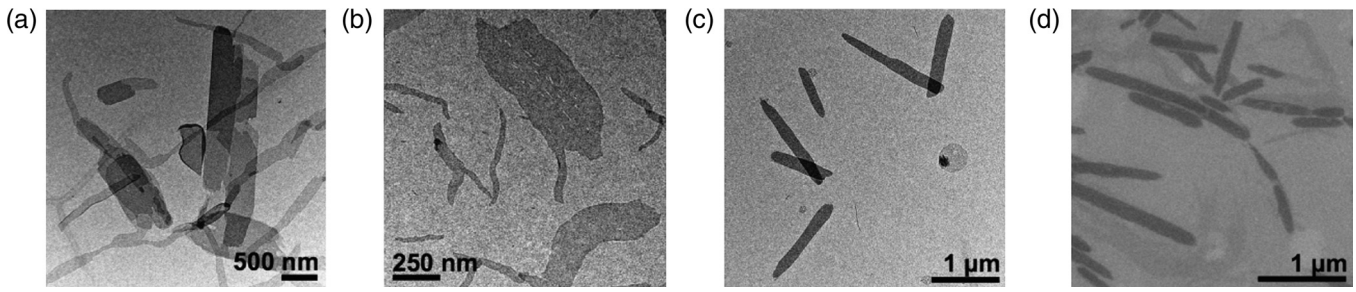

Figure 8 | *TEM and SEM images of the nanoplates prepared in 70%* n*-hexane–acetone mixture from (a)* ***3*** *(2 × 10^{-4} M); (b)* ***4*** *(2 × 10^{-4} M) and (c, d)* ***5*** *(2 × 10^{-4} M).*

DOI: 10.31635/ccschem.019.20190041
CCS Chem. **2019**, *1*, 464–475

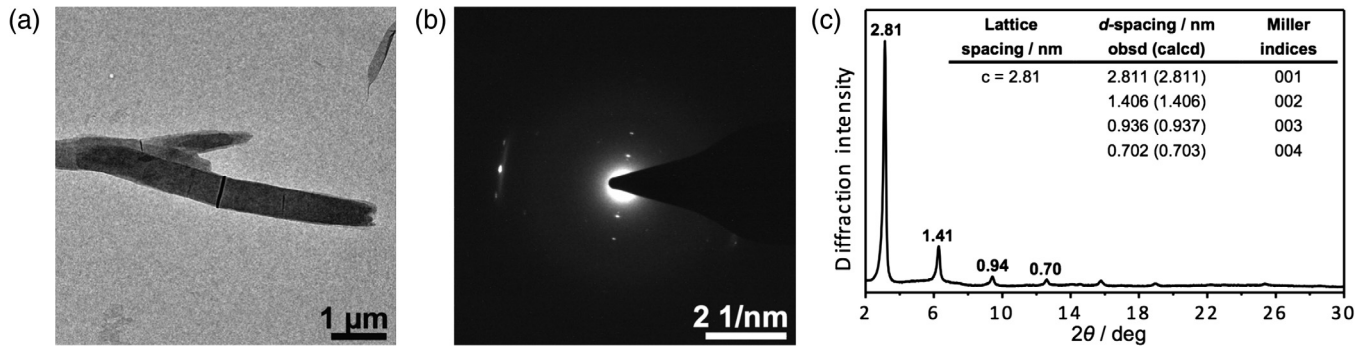

Figure 9 | *(a) TEM images of the superstructures prepared from* ***5*** *(2×10^{-4} M) in 70%* n*-hexane–acetone mixture. (b) The corresponding SAED pattern of a single nanoplate. (c) XRD patterns obtained from powder sample prepared from* ***5*** *in 70%* n*-hexane–acetone mixture. Numerical values represent* d*-spacing (in nanometers).*

media. We proposed that the alkynylplatinum(II) complexes were stacked into a lamellar packing with interlamellar separation of ~ 2.8 nm orthogonal to the nanoplate long axis, comparable to the simulated molecular length of **5** (~ 2.63 nm; Supporting Information Figure S14). The intralamellar separation along the nanoplate long axis was determined to be ~ 0.32 nm, attributed to the Pt···Pt and/or π–π stacking interactions along this long axis. Such molecular association process could be rationalized by the reduced solvation of the cationic charged platinum(II) complex in a nonpolar condition that led to the formation of Pt···Pt interactions in stabilizing the planar conformation of the aggregates. The twisted nanofibrils in aqueous media, on the other hand, could be ascribed to the molecular association of the cyclosiloxane motifs through hydrophobic interactions, which further brought the platinum(II) terpyridine moieties into proximity, giving rise to the Pt···Pt interactions and the associated spectroscopic changes. Collectively, these studies illustrate that the change of solvent polarity could have a tremendous influence on perturbation of the supramolecular architectures through manipulation of the hydrophobic and Pt···Pt interactions.

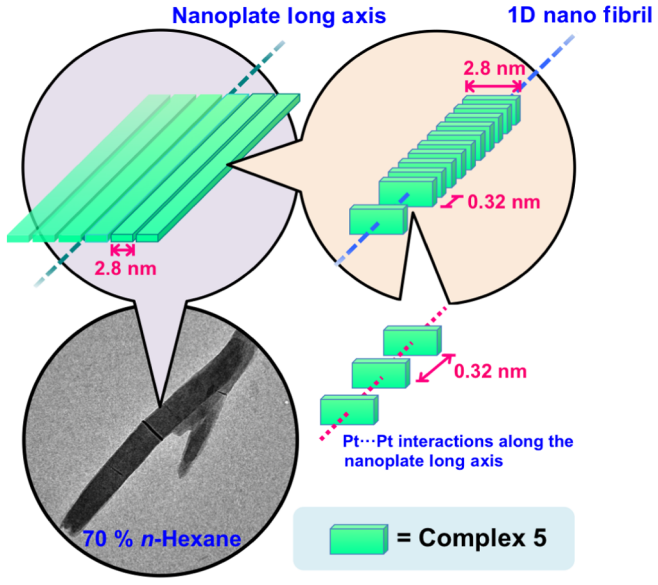

Figure 10 | *Schematic illustration of the proposed structure of the nanoplates prepared from* ***5*** *in 70%* n*-hexane–acetone mixture.*

Solvent-Dependent Supramolecular Polymerization Mechanism

We studied the mechanism for the solvent-induced self-assembly of **4**–**6**. A plot of the degree of aggregation against various solvent systems demonstrated solvent dependence of the association mechanism in the current system. The underlying thermodynamic parameters of the supramolecular self-assembly process of **4** in *n*-hexane–acetone media were obtained using the nucleation–elongation model developed by Meijer[42] through the fitting of the corresponding plot of the degree of aggregation against solvent composition to rationalize the thermodynamic exhibitions (Supporting Information Figure S15). A sigmoidal curve with ΔG^0 value of ~ –36 kJ·mol^{-1} was obtained, suggesting an isodesmic molecular association mechanism. Similar studies were carried out for complexes **5** and **6** (Supporting Information Figures S16 and S17), which also displayed an isodesmic growth mechanism with the thermodynamic parameters summarized in Table 1. Complex **5** exhibited a more negative ΔG^0 value of ~ –44 kJ·mol^{-1}, indicating a more favorable molecular association process in **5**, compared with that observed in **4**. Such phenomenon could probably be ascribed to the presence of a twisted phenyl moiety[43,44] on the terpyridine system in **4**, potentially hindering the self-assembly processes, whereas the absence of the phenyl moiety in the analogue complex **5** potentially led to a better degree of

DOI: 10.31635/ccschem.019.20190041
CCS Chem. **2019**, *1*, 464–475

Table 1 | *Thermodynamic Parameters of* ***4–6*** *in* n-*Hexane–Acetone Media at 298 K*

Complexes	ΔG^0/kJ·mol^{-1}	m/kJ·mol^{-1}
4	−36.1 ± 1.3	38.4 ± 3.4
5	−44.5 ± 1.0	53.4 ± 2.5
6	−50.1 ± 1.6	42.3 ± 2.4

Pt···Pt and/or π–π stacking interactions, which favored the association process. Further introduction of cationic domains into the system in **6** also resulted in a more favorable assembly process, with ΔG^0 value of approximately −50 kJ·mol^{-1}, which could be attributable to the presence of unfavorable interactions among the cationic domains and the nonpolar solvent, generally promoting the aggregated state, potentially acting as an additional driving force toward the assembly process.

In addition to understanding the molecular association processes in nonpolar solvents, the self-assembly properties in aqueous media were explored. It is interesting to note that corresponding plots of the degree of aggregation against aqueous composition for **4–6** exhibited considerable abrupt changes in response to the addition of water, representing nonsigmoidal changes in response to changes in proportions of solvent compositions. Attempts to fit the data into the isodesmic model yielded significantly poor description of the data, potentially revealing a cooperative character of the growth mechanism. Attempts to cooperatively fit the data into the nucleation–elongation model were unsuccessful owing to the limited temperature range for the corresponding temperature-dependent studies in acetone mixtures for the determination of the nucleus size (*n*) of the cooperative mechanism.

Although extraction of quantitative data from the nucleation–elongation model for the cooperative mechanism was not feasible in aqueous media, we still can obtain general insights toward the assembly mechanism: Complexes **4–6** exhibited different growth mechanisms in response to solvent polarities. Isodesmic growth mechanisms were demonstrated in a polar environment, while the assembly processes in nonpolar media are found to be cooperative. The cooperative growth in aqueous condition was attributable to the cooperative nature of the hydrophobic interactions,[45–47] arising from the collective interactions among the hydrogen bond networks that surrounded the hydrophobic domains[45]; though a synergistic effect of hydrophobic interactions together with metal–metal interactions could not be ruled out.[48] In contrast to the molecular association process in polar media, isodesmic growth mechanism in nonpolar environment was observed and was attributed to the absence of cooperative hydrophobic interactions, with the Pt···Pt and/or π–π stacking interactions as the only dominating driving forces toward the molecular association processes.

Effect of Charged Moieties on the Self-Assembly Behavior

Complex **5** displayed aggregation behaviors in nonpolar media; the driving force was reduced solvation of the cationic charged platinum(II) terpyridine moiety. As an extension of such studies, additional charged moieties were incorporated into the system and we synthesized complex **6** with significantly enhanced charged density. We envisaged that with the introduction of the charged moieties, the aggregation ability in nonpolar media could be promoted further, while self-assembly behaviors in polar media could also be altered. In addition, the solvent-dependent properties, as well as supramolecular assembly properties were investigated.

In contrast to the analogue complex **5**, solvent-dependent electronic absorption studies of **6** (Supporting Information Figure S7) displayed a significantly blue-shifted MMLCT absorption band (500 nm, shoulder) upon increasing the water composition in acetone media, which could possibly be attributed to the weakening of Pt···Pt and/or π–π stacking interactions derived from the reduced aggregation in polar media. This finding was consistent with the amount of water required to trigger the MMLCT transition band, with complex **6** showing a significantly higher critical solvent composition of ~ 70% water (Supporting Information Figure S7), compared with corresponding studies of complex **5**, which revealed a much lower critical water composition of ~ 40%. The critical solvent composition required to trigger the molecular association process was found to be thermodynamically related,[42] with a smaller value representing a more favorable aggregation process. Thus, the higher critical solvent composition of **6** revealed its smaller tendency toward molecular association, which could be rationalized by the improved solvation of the complexes in polar media through the additional introduction of charged moieties.

Furthermore, we investigated the effects of solvent polarity on the aggregation process through solvent-dependent electronic absorption studies with the gradual addition of nonpolar solvents *n*-hexane. Corresponding electronic absorption spectra of **6** in acetone revealed the development of a low-energy MMLCT absorption tail at ~ 590 nm upon raising the *n*-hexane content. The corresponding plot of absorbance against *n*-hexane content revealed that a critical solvent composition of ~ 30% was required to initiate the molecular association process (Figure 6), which was significantly lower than that for the analogue complex **5**. Such finding was in accordance with that observed in polar media and

DOI: 10.31635/ccschem.019.20190041
CCS Chem. **2019**, *1*, 464–475

could be attributable to the introduction of charged motifs that significantly reduced the complex solvation in nonpolar media, posing additional driving forces for the aggregation process. Further evidence for the molecular association processes came from the corresponding solvent-dependent emission studies, which revealed a drop in the ^{3}MLCT emission band at 600 nm and a concomitant growth of the near-IR ^{3}MMLCT emission band at ~ 748 nm (Figure 6b), suggesting the formation of Pt···Pt and/or π–π stacking interactions resulting from molecular association at increasing *n*-hexane content.

Finally, we investigated the solvent-dependent molecular association processes by electron microscopy. The corresponding TEM images of **6** in 70% *n*-hexane–acetone mixture revealed short fibers of a few microns long and ~ 20 nm wide (Supporting Information Figure S18), further supporting the formation of aggregated species in nonpolar media. Notably, the electron micrographs of **6** in 70% water–acetone system revealed the absence of distinct nanostructures, indicating a lesser extent of aggregation, which, possibly was due to the improved solvation of high-aqueous media content owing to the introduction of the charged units. However, the possibility of coulombic repulsion leading to an inhibition of aggregation could not be excluded completely.

Conclusions

We have synthesized and characterized a series of cyclotetrasiloxane–functionalized alkynylplatinum(II) terpyridine complexes. Examination of their self-association mechanisms and the underlying thermodynamic parameters revealed that changing solvent compositions cast a profound impact on the morphologies of the nanostructures. We identified twisted fibrils in aqueous acetone, while plate-like assemblies were observed in the *n*-hexane–acetone mixture, indicative of similar molecular packing conformations among the complexes in response to different solvent microenvironments. Corresponding studies, using the nucleation–elongation model, revealed cooperative growth mechanisms with complexes **4**–**6** in aqueous media, attributable to the cooperative nature of the hydrophobic interactions. In contrast, isodesmic growth mechanisms were demonstrated in nonpolar media, revealing the isodesmic nature of the Pt···Pt and/or π–π stacking interactions in such system.

Supporting Information

Supporting Information is available.

Conflicts of Interest

There are no conflicts to declare.

DOI: 10.31635/ccschem.019.20190041
CCS Chem. **2019**, *1*, 464–475

Acknowledgments

V.W.-W. Y. acknowledges the University Grants Committee (UGC) funding administered by The University of Hong Kong for supporting the Electrospray Ionization Quadrupole Time-of-Flight (ESI-TOF) Mass Spectrometry Facilities under the Support for Interdisciplinary Research in Chemical Science, and the support from the University Research Committee (URC) Strategically Oriented Research Theme (SORT) on Functional Materials for Molecular Electronics. This work was also supported by the University Grants Committee Areas of Excellence (AoE) Scheme (AoE/P-03/08), and a General Research Fund (GRF) grant from the Research Grants Council of Hong Kong Special Administrative Region, P.R. China (HKU 17304715).

References

1. Williams, J. A. G. Photochemistry and Photophysics of Coordination Compounds: Platinum. In *Photochemistry and Photophysics of Coordination Compounds II. Topics in Current Chemistry*; Balzani, V., Campagna, S., Eds.; Springer: Berlin, Heidelberg, **2007**; Vol. 281.
2. Mason, W. R.; Gray, H. B. Electronic Structures of Square-Planar Complexes. *J. Am. Chem. Soc.* **1968**, *90*, 5721–5729.
3. Gliemann, G.; Yersin, H. Spectroscopic Properties of the Quasi One-Dimensional Tetracyanoplatinate(II) Compounds. In Clarke, M. J.; Goodenough, J. B.; Ibers, J. A.; Jørgensen, C. K.; Mingos, D. M. P.; Neilands, J. B.; Palmer, G. A.; Reinen, D.; Sadler, P. J.; Weiss, R.; Williams, R. J. P., Eds. *Clusters. Structure and Bonding*; Springer, Berlin, Heidelberg, **1985**; Vol. 62.
4. Schindler, J. W.; Fukuda, R. C.; Adamson, A. W. Photophysics of Aqueous $Pt(CN)_4^{2-}$. *J. Am. Chem. Soc.* **1982**, *104*, 3596–3600.
5. Atoji, M.; Richardson, J. W.; Rundle, R. E. On the Crystal Structures of the Magnus Salts, $Pt(NH_3)_4PtCl_4$. *J. Am. Chem. Soc.* **1957**, *79*, 3017–3020.
6. Bally, J. A.; Miskowski, V. M.; Gray, H. B. Spectroscopic and Structural Properties of Binuclear Platinum–Terpyridine Complexes. *Inorg. Chem.* **1993**, *32*, 369–370.
7. Yip, H.-K.; Cheng, L.-K.; Cheung, K.-K.; Che, C.-M. Luminescent Platinum(II) Complexes. Electronic Spectroscopy of Platinum(II) Complexes of 2,2′:6″,2″-Terpyridine(terpy) and p-Substituted Phenylterpyridines and Crystal Structure of $[Pt(terpy)Cl][CF_3SO_3]$. *J. Chem. Soc., Dalton Trans.* **1993**, 2933–2938.
8. Yam, V. W.-W.; Wong, K. M.-C.; Zhu, N. Solvent-Induced Aggregation Through Metal···Metal/π···π Interactions: Large Solvatochromism of Luminescent Organoplatinum(II) Terpyridyl Complexes. *J. Am. Chem. Soc.* **2002**, *124*, 6506–6507.
9. Tam, A. Y.-Y.; Wong, K. M.-C.; Wang, G.; Yam, V. W.-W. Luminescent Metallogels of Platinum(II) Terpyridyl

Complexes: Interplay of Metal···Metal, π–π and Hydrophobic–Hydrophobic Interactions on Gel Formation. *Chem. Commun.* **2007**, 2028–2030.
10. Leung, S. Y.-L.; Wong, K. M.-C.; Yam, V. W.-W. Self-Assembly of Alkynylplatinum(II) Terpyridine Amphiphiles into Nanostructures via Steric Control and Metal–Metal Interactions. *Proc. Natl. Acad. Sci. U.S.A.* **2016**, *113*, 2845–2850.
11. Yam, V. W.-W.; Tang, R. P.-L.; Wong, K. M.-C.; Cheung, K.-K. Synthesis, Luminescence, Electrochemistry, and Ion-Binding Studies of Platinum(II) Terpyridyl Acetylide Complexes. *Organometallics* **2001**, *20*, 4476–4482.
12. Connick, W. B.; Marsh, R. E.; Schaefer, W. P.; Gray, H. B. Linear-Chain Structures of Platinum(II) Diimine Complexes. *Inorg. Chem.* **1997**, *36*, 913–922.
13. Miskowski, V. M.; Houlding, V. H. Electronic Spectra and Photophysics of Platinum(II) Complexes With α-Diimine Ligands. Solid-State Effects. 1. Monomers and Ligand π Dimers. *Inorg. Chem.* **1989**, *28*, 1529–1533.
14. Miskowski, V. M.; Houlding, V. H. Electronic Spectra and Photophysics of Platinum(II) Complexes With α-Diimine Ligands. Solid-State Effects. 2. Metal–Metal Interaction in Double Salts and Linear Chains. *Inorg. Chem.* **1991**, *30*, 4446–4452.
15. Aldridge, T. K.; Stacy, E. M.; McMillin, D. R. Studies of the Room-Temperature Absorption and Emission Spectra of $[Pt(trpy)X]^+$ Systems. *Inorg. Chem.* **1994**, *33*, 722–727.
16. Yam, V. W.-W.; Tang, R. P.-L.; Wong, K. M.-C.; Cheung, K.-K. Synthesis, Luminescence, Electrochemistry, and Ion-Binding Studies of Platinum(II) Terpyridyl Acetylide Complexes. *Organometallics* **2001**, *20*, 4476–4482.
17. Connick, W. B.; Marsh, R. E.; Schaefer, W. P.; Gray, H. B. Two Compounds Containing the Tris(μ-chloro) hexakis(tetrahydrofuran)divanadium(II) Cation. Preparation, Structures, and Spectroscopic Characterization. *Inorg. Chem.* **1997**, *36*, 913–917.
18. Miskowski, V. M.; Houlding, V. H.; Che, C. M.; Wang, Y. Electronic Spectra and Photophysics of Platinum(II) Complexes With α-Diimine Ligands. Mixed Complexes With Halide Ligands. *Inorg. Chem.* **1993**, *32*, 2518–2524.
19. Chan, A. K.-W.; Yam, V. W.-W. Precise Modulation of Molecular Building Blocks From Tweezers to Rectangles for Recognition and Stimuli-Responsive Processes. *Acc. Chem. Res.* **2018**, *51*, 3041–3051.
20. Wong, Y.-S.; Leung, F. C.-M.; Ng, M.; Cheng, H.-K.; Yam, V. W.-W. Platinum(II)-Based Supramolecular Scaffold-Templated Side-by-Side Assembly of Gold Nanorods Through Pt···Pt and π–π Interactions. *Angew. Chem. Int. Ed.* **2018**, *57*, 15797–15801.
21. Chan, M. H.-Y.; Leung, S. Y.-L.; Yam, V. W.-W. Controlling Self-Assembly Mechanisms Through Rational Molecular Design in Oligo(p-phenyleneethynylene)-Containing Alkynylplatinum(II) 2,6-Bis(N-alkylbenzimidazol-2′-yl)pyridine Amphiphiles. *J. Am. Chem. Soc.* **2018**, *140*, 7637–7646.
22. Lippard, S. J. Platinum Complexes: Probes of Polynucleotide Structure and Antitumor Drugs. *Acc. Chem. Res.* **1978**, *11*, 211–217.
23. Herber, R. H.; Croft, M.; Coyer, M. J.; Bilash, B.; Sahiner, A. Origin of Polychromism of Cis Square-Planar Platinum(II) Complexes: Comparison of Two Forms of $[Pt(2,2'\text{-bpy})(Cl)_2]$. *Inorg. Chem.* **1994**, *33*, 2422–2426.
24. Bailey, J. A.; Hill, M. G.; Marsh, R. E.; Miskowski, V. M.; Schaefer, W. P.; Gray, H. B. Electronic Spectroscopy of Chloro(terpyridine)platinum(II). *Inorg. Chem.* **1995**, *34*, 4591–4599.
25. Hill, M. G.; Bailey, J. A.; Miskowski, V. M.; Gray, H. B. Spectroelectrochemistry and Dimerization Equilibria of Chloro(terpyridine)platinum(II). Nature of the Reduced Complexes. *Inorg. Chem.* **1996**, *35*, 4585–4590.
26. Panisch, R.; Bassindale, A. R.; Korlyukov, A. A.; Pitak, M. B.; Coles, S. J.; Taylor, P. G. Selective Derivatization and Characterization of Bifunctional "Janus-Type" Cyclotetrasiloxanes. *Organometallics* **2013**, *32*, 1732–1742.
27. Frampton, M. B.; Marquardt, D.; Jones, T. R. B.; Harroun, T. A.; Zelisko, P. M. Macrocyclic Oligoesters Incorporating a Cyclotetrasiloxane Ring. *Biomacromolecules* **2015**, *16*, 2091–2100.
28. Cordes, D. B.; Lickiss, P. D.; Rataboul, F. Recent Developments in the Chemistry of Cubic Polyhedral Oligosilsesquioxanes. *Chem. Rev.* **2010**, *110*, 2081–2173.
29. Wu, J.; Mather, P. T. POSS Polymers: Physical Properties and Biomaterials Applications. *Polym. Rev.* **2009**, *49*, 25–63.
30. Brown, J. F.; Slusarczhuk, G. M. J. Macrocyclic Polydimethylsiloxanes. *J. Am. Chem. Soc.* **1965**, *87*, 931–932.
31. Seyferth, D.; Prud'homme, C.; Wiseman, G. H. Cyclic Polysiloxanes From the Hydrolysis of Dichlorosilane. *Inorg. Chem.* **1983**, *22*, 2163–2167.
32. Casado, C. M.; Cuadrado, I.; Morán, M.; Alonso, B.; Barranco, M.; Losada, J. Cyclic Siloxanes and Silsesquioxanes as Cores and Frameworks for the Construction of Ferrocenyl Dendrimers and Polymers. *Appl. Organomet Chem.* **1999**, *13*, 245–259.
33. Wei, K.; Wang, L.; Zheng, S. Organic–Inorganic Polyurethanes With 3,13-Dihydroxypropyloctaphenyl Double-Decker Silsesquioxane Chain Extender. *Polym. Chem.* **2013**, *4*, 1491–1501.
34. Feher, F. J.; Wyndham, K. D. Amine and Ester-Substituted Silsesquioxanes: Synthesis, Characterization and Use as a Core for Starburst Dendrimers. *Chem. Commun.* **1998**, *3*, 323–324.
35. Wong, K. M.-C.; Tang, W.-S.; Chu, B. W.-K.; Zhu, N.; Yam, V. W.-W. Synthesis, Photophysical Properties, and Biomolecular Labeling Studies of Luminescent Platinum(II)–Terpyridyl Alkynyl Complexes. *Organometallics* **2004**, *23*, 3459–3465.
36. Yam, V. W.-W.; Chan, K. H.-Y.; Wong, K. M.-C.; Chu, B. W.-K. Luminescent Dinuclear Platinum(II) Terpyridine Complexes With a Flexible Bridge and "Sticky Ends". *Angew. Chem. Int. Ed.* **2006**, *45*, 6169–6173.
37. Yu, C.; Chan, K. H.-Y.; Wong, K. M.-C.; Yam, V. W.-W. Single-Stranded Nucleic Acid-Induced Helical Self-Assembly of Alkynylplatinum(II) Terpyridyl Complexes. *Proc. Natl. Acad. Sci. U.S.A.* **2006**, *103*, 19652–19657.
38. Yu, C.; Chan, K. H.-Y.; Wong, K. M.-C.; Yam, V. W.-W. Polyelectrolyte-Induced Self-Assembly of Positively

DOI: 10.31635/ccschem.019.20190041
CCS Chem. **2019**, *1*, 464–475

Charged Alkynylplatinum(II)–Terpyridyl Complexes in Aqueous Media. *Chem. Eur. J.* **2008**, *14*, 4577–4584.
39. Po, C.; Tam, A. Y.-Y.; Wong, K. M.-C.; Yam, V. W.-W. Supramolecular Self-Assembly of Amphiphilic Anionic Platinum(II) Complexes: A Correlation Between Spectroscopic and Morphological Properties. *J. Am. Chem. Soc.* **2011**, *133*, 12136–12143.
40. Au-Yeung, H.-L.; Tam, A. Y.-Y.; Leung, S. Y.-L.; Yam, V. W.-W. Supramolecular Assembly of Platinum-Containing Polyhedral Oligomeric Silsesquioxanes: An Interplay of Intermolecular Interactions and a Correlation Between Structural Modifications and Morphological Transformations. *Chem. Sci.* **2017**, *8*, 2267–2276.
41. Huang, M. H.; Kartono, F.; Dunn, B.; Zink, J. I.; Valverde, G.; García, J. Hexagonal to Lamellar Mesostructural Changes in Silicate Films Caused by Organic Additives. *Chem. Mater.* **2002**, *14*, 5153–5162.
42. Korevaar, P. A.; Schaefer, C.; de Greef, T. F. A.; Meijer, E. W. Controlling Chemical Self-Assembly by Solvent-Dependent Dynamics. *J. Am. Chem. Soc.* **2012**, *134*, 13482–13491.
43. Brock, C. P.; Minton, R. P. Systematic Effects of Crystal-Packing Forces: Biphenyl Fragments With Hydrogen Atoms in All Four Ortho Positions. *J. Am. Chem. Soc.* **1989**, *111*, 4586–4593.
44. Göller, A.; Grummt, U. W. Torsional Barriers in Biphenyl, 2,2′-Bipyridine and 2-Phenylpyridine. *Chem. Phys. Lett.* **2000**, *321*, 399–405.
45. Jiang, L.; Cao, S.; Cheung, P. P.-H.; Zheng, X.; Leung, C. W. T.; Peng, Q.; Shuai, Z.; Tang, B. Z.; Yao, S.; Huang, X. Real-Time Monitoring of Hydrophobic Aggregation Reveals a Critical Role of Cooperativity in Hydrophobic Effect. *Nat. Commun.* **2017**, *8*, 15639.
46. Wang, L., Friesner, R. A.; Berne, B. J. Hydrophobic Interactions in Model Enclosures From Small to Large Length Scales: Non-Additivity in Explicit and Implicit Solvent Models. *Faraday Discuss.* **2010**, *146*, 247–262.
47. Shimizu, S.; Chan, H. S. Anti-Cooperativity and Cooperativity in Hydrophobic Interactions: Three-Body Free Energy Landscapes and Comparison With Implicit-Solvent Potential Functions for Proteins. *Proteins* **2002**, *48*, 15–30.
48. Chan, A. K.-W.; Wong, K. M.-C.; Yam, V. W.-W. Supramolecular Assembly of Isocyanorhodium(I) Complexes: An Interplay of Rhodium(I)···Rhodium(I) Interactions, Hydrophobic–Hydrophobic Interactions, and Host–Guest Chemistry. *J. Am. Chem. Soc.* **2015**, *137*, 6920–6931.